

Adsorption of HCl on the Water Ice Surface Studied by X-ray Absorption Spectroscopy

Ph. Parent^{*,†} and C. Laffon^{*,†,‡}

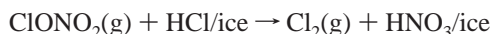
Laboratoire pour l'Utilisation du Rayonnement Electromagnétique (LURE), Centre Universitaire de Paris-Sud, BP 34, 91898 Orsay Cedex, France, and Laboratoire de Chimie Physique-Matière et Rayonnement (LCP-MR), Université Pierre-et-Marie Curie et CNRS, 11 rue Pierre-et-Marie Curie, 75005 Paris Cedex 05, France

Received: July 30, 2004; In Final Form: October 29, 2004

The adsorption state of HCl at 20 and 90 K on crystalline water ice films deposited under ultrahigh vacuum at 150 K has been studied by X-ray absorption spectroscopy at the O1s K-edge and Cl2p L-edge. We show that HCl dissociates at temperatures as low as 20 K, in agreement with the prediction of a spontaneous ionization of HCl on ice. Comparison between the rate of saturation of the “dangling” hydrogen bonds and the chlorine uptake indicates that hydrogen bonding of HCl with the surface native water “dangling” groups only accounts for a small part of the ionization events (20% at 90 K). A further mechanism drives the rest of the dissociation/solvation process. We suggest that the weakening of the ice surface hydrogen-bond network after the initial HCl adsorption phase facilitates the generation of new dissociation/solvation sites, which increases the uptake capacity of ice. These results also emphasize the necessity to take into account not only a single dissociation event but its catalyzing effect on the subsequent events when modeling the uptake of hydrogen-bonding molecules on the ice surface.

1. Introduction

It is well-established that chlorine activation on icy polar stratospheric clouds (PSCs) plays a key role in the seasonal depletion of the stratospheric ozone layer.^{1–3} Most of the chlorine chemistry occurs in heterogeneous reactions between inert chlorinated molecules and acidified PSCs surface, leading to the liberation of active molecular Cl₂, as for instance in the reaction:



Understanding the molecular mechanisms of such reactions requires a detailed characterization of the interaction of HCl with ice. This has recently been the focus of considerable attention, using theoretical approaches^{4–13} or laboratory experiments.^{14–33} Recent results show that at submonolayer coverage and tens of degrees kelvin, molecular HCl can exist at the surface of ice, in coexistence with ionized HCl.^{14–16,18,19,24,33} Kang et al.²⁴ have studied the adsorption of HCl on ice films grown under UHV conditions from 50 to 140 K at low acid exposure. Both ionized and molecular HCl are present, their proportion varying with temperature. HCl adsorbs molecularly at 50 K but dissociates when the surface temperature rises, indicating that the ionization rate has some thermal dependence. However, at a molecular scale, many calculations predict that the elementary dissociation mechanism of HCl on ice is not thermally activated.^{4,9–13,18,19} In these models, the number of “dangling” water molecules³⁴ at the adsorption sites is a key property for ionization. It is frequently reported that three hydrogen bonds (H-bonds) between HCl and the surface dangling groups are required, and such favorable sites on the ice surface are found on top of the center of the hexagon of the

ice Ih[0001] basal plane^{9,10,12,13} or at defective sites.¹¹ Other models predict an efficient solvation of the Cl[−] ion when it is included in the first ice layer, either directly by adsorption into a water vacancy^{5,35,36} or because further water molecules adsorb on HCl, dissociating the molecule and solvating the anion.⁴ Those processes are favored by a high surface temperature³⁶ or high water partial pressure,⁴ providing a plausible mechanism for the increasing HCl ionization rate with the surface temperature observed in most of the experiments published so far.^{18,19,24} However, the presence of chloride ion Cl[−] has been reported for temperatures as low as 50 K by FTIR on ice nanocrystal arrays,^{14,18,19} in good agreement with the prediction of a nonthermal ionization reaction.^{9–11}

To ascertain the role of the ice surface temperature on the ionization rate of HCl, and with the aim of improving our understanding of this reaction on a molecular scale, we have undertaken the study of HCl condensed at 20 and 90 K on crystalline ice films, two temperatures below the penetration threshold of HCl into crystalline ice (we found around 120 K).³⁷ We have used X-ray absorption spectroscopy (or NEXAFS, for near-edge X-ray absorption fine structures) at the Cl2p and O1s edges, in conventional mode, that probes the bulk of ice, and the photo-stimulated desorption technique (PSD-NEXAFS), which is sensitive only to the top layer of the surface.

2. Experimental Method

The NEXAFS measurements have been done on the SACEMOR experimental setup on the SM-PGM monochromator of the SuperACO SA22 beamline (LURE, Orsay), with a resolving power better than 5000. The energy was calibrated at the Cl2p and the O1s edges using the absorption features of the first-order K excitation of the oxygen species contaminating the optics. The NEXAFS spectra have been recorded in total electron yield (TEY), by calculating the ratio of the photocurrent of the sample vs that of the beam monitor. The PSD-NEXAFS measurements were recorded in total ion yield (TIY), using a

* Corresponding authors. E-mail: Philippe.Parent@lure.u-psud.fr (P.P.); Carine.Laffon@lure.u-psud.fr (C.L.).

[†] Centre Universitaire de Paris-Sud.

[‡] Université Pierre-et-Marie Curie et CNRS.

20 cm² two-stages microchannel plate (BURLE) biased at -2.0 kV, and the spectra are the ratio of the sample total ion yield on the beam monitor photocurrent. After the ultrapure H₂O was degassed by several freeze–pump–thaw cycles, crystalline ice films were prepared by dosing 100 langmuir (1 langmuir = 1×10^{-6} Torr s) of H₂O vapor at a rate of 0.1 langmuir s⁻¹ on a clean Au(111) single crystal at 150 K, using a diffuser outlet located at the back of the substrate (background dosing). This was done in a special chamber separated from the main measurement chamber (base pressure 5×10^{-11} Torr in both) to avoid further exposure during the analysis. The substrate temperature was measured using a platinum resistance clamped on the back of the crystal. Assuming a sticking coefficient of unity for the molecular condensation of ice at 150 K,³⁸ 1 langmuir is equivalent to a coverage of 1 monolayer (ML), and the films are therefore 100 ML thick (about 270 Å thick; the depth probed with NEXAFS is about 50 Å). The films were cooled and maintained at 20 or 90 K for the HCl exposures (Air Liquide, electronic grade) in the preparation chamber, dosed from the background using a circuitry different from that of H₂O, to avoid any hydration of HCl in the gas line prior to the deposit. HCl exposures are given in langmuir after correction for the gauge ionization efficiency, which is 1.6 times more sensitive for HCl than for water or nitrogen.³⁹ The PSD and TEY NEXAFS spectra were collected simultaneously, at the temperature of the dosings, i.e., 20 or 90 K. The HCl multilayer condensation is possible at 20 K but not at 90 K (we found the condensation point at 72 K).

In a conventional NEXAFS experiment, the data are usually recorded in TEY mode by measuring the yield of primary Auger or secondary electrons emitted by the electronic relaxation of the core hole as a function of the energy of the incident X-ray photons across a photoexcitation threshold. The TEY spectrum is representative of the bulk of the film (~ 50 Å) due to the large escape depth of the Auger/secondary electrons. In the PSD mode, we detect the ions (for ice, essentially H⁺⁴⁰) emitted in the vacuum by fragmentations of the core excited molecules.⁴¹ Contrary to electrons, the ions have very low kinetic energies, and they are readily stopped by inelastic collisions. Only those emitted at the very surface are able to escape, and the PSD signal is representative of the top surface layer (~ 2 Å). In the following, we call the normal bulk NEXAFS signal “NEXAFS” or “TEY” and the PSD-NEXAFS surface signal “PSD”.

3. Results

(a) The Cl₂p Spectra of HCl and Cl⁻. The Cl₂p NEXAFS spectra of ionized and molecular HCl are strongly different.^{37,42} Figure 1 shows the Cl₂p NEXAFS spectrum of HCl (curve 1), measured on molecular hydrogen chlorine condensed at 50 K (45 langmuir exposure), compared with that of the chloride anion Cl⁻ (curve 3) obtained by the adsorption of 1 langmuir of HCl at 120 K on a crystalline water ice film.⁴² On HCl, resonance M at 201 eV is the Cl₂p transition to the $\sigma^*(\text{H}-\text{Cl})$ orbital, followed by the 4s Rydberg state at 203.3 eV. Resonance M is a signature of the H–Cl bond and is thus related to the molecular character of HCl. For the Cl⁻ anion, the H–Cl bond does not exist and the $\sigma^*(\text{H}-\text{Cl})$ resonance is not observed. We see the 4s Rydberg state of Cl⁻ (labeled I) shifted down to 200.1 eV, the negative charge of the anion lowering its ionization potential. Thus, the absence of M and the presence of I are evidence of the ionization of HCl. Last, the broad resonance at 213.7 eV in HCl and 216 eV in Cl⁻ (labeled E and E', respectively) results from the backscattering of the photoelectron on the neighboring molecules. This resonance is not at the same energy in HCl

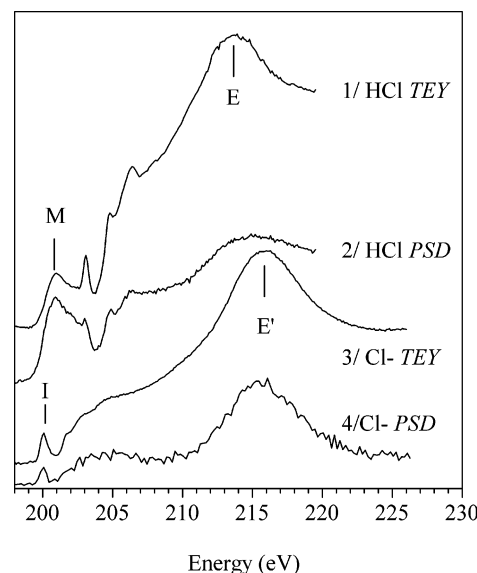


Figure 1. Cl₂p NEXAFS spectra of molecular HCl, measured on 45 langmuir of pure HCl condensed at 50 K, recorded in (1) TEY (bulk signal) and (2) PSD (surface signal). Cl₂p NEXAFS spectra of chloride anion Cl⁻, obtained by the adsorption of 1 langmuir of HCl condensed at 120 K on a crystalline water ice film (100 langmuir deposited at 150 K), recorded in (3) TEY (bulk signal) and (4) PSD (surface signal).

and Cl⁻, because chlorine has a different structural environment in the two cases.⁴³

Figure 1 also shows the Cl₂p PSD signals of HCl and Cl⁻ (curve 2 and 4, respectively). On HCl, the surface signal (curve 2) essentially resembles the bulk (curve 1), the small differences being related to small structural variations between the bulk and the surface and to the detection methods.⁴² Indeed, the PSD technique enhances the $\sigma^*(\text{H}-\text{Cl})$ resonance due to the high fragmentation yield of the H–Cl bond at the Cl₂p excitation.⁴⁴ PSD is therefore very sensitive to molecular HCl, and we will use this advantage to detect traces of HCl on ice. Concerning the Cl⁻ PSD data (curve 4), the anions remain at the top layer and do not penetrate into the water ice film, as shown later. The NEXAFS (curve 3) and the PSD signal (curve 4) both come from the surface and have about the same shape.

(b) HCl on Ice at 20 and 90 K: Cl₂p Results. TEY. Figure 2 shows the Cl₂p TEY for increasing HCl exposures at 90 K (Figure 2 A) and 20 K (Figure 2 B) on ice. We have stopped the dosings around 40–50 langmuir, when no further evolution in shape and intensity is observed. For clarity, the low-energy range (198–204 eV) is magnified to enhance the low-exposure data, and the high-energy part (204–222 eV) is rescaled to match the intensities at the break point (204 eV).

At 90 K, only Cl⁻ is observed and no molecular HCl is detected in the whole exposure range. HCl is therefore fully ionized at 90 K. At 20 K and at low exposures (0.1–1 langmuir), resonance I of Cl⁻ and the presence of E' show that HCl is ionized. Above 1 langmuir, the increase of M and of the 4s transition, as well as the continuous transition from E' to E, shows that a molecular layer condenses on top of the first ionized layer.

PSD. Figure 3 shows the corresponding PSD spectra. At 20 K (Figure 3 A) the PSD signal is mostly dominated by molecular HCl, with some Cl⁻ detected at 0.1 and 0.3 langmuir (resonance I), screened by HCl at higher exposures. The contrast between the TEY (where only Cl⁻ is observed, Figure 2 B) and the PSD is due to the higher sensitivity of the PSD technique to molecular HCl. The PSD signal of Figure 3A is essentially produced by the few HCl adsorbed at the side of the Cl⁻ ions; these HCl

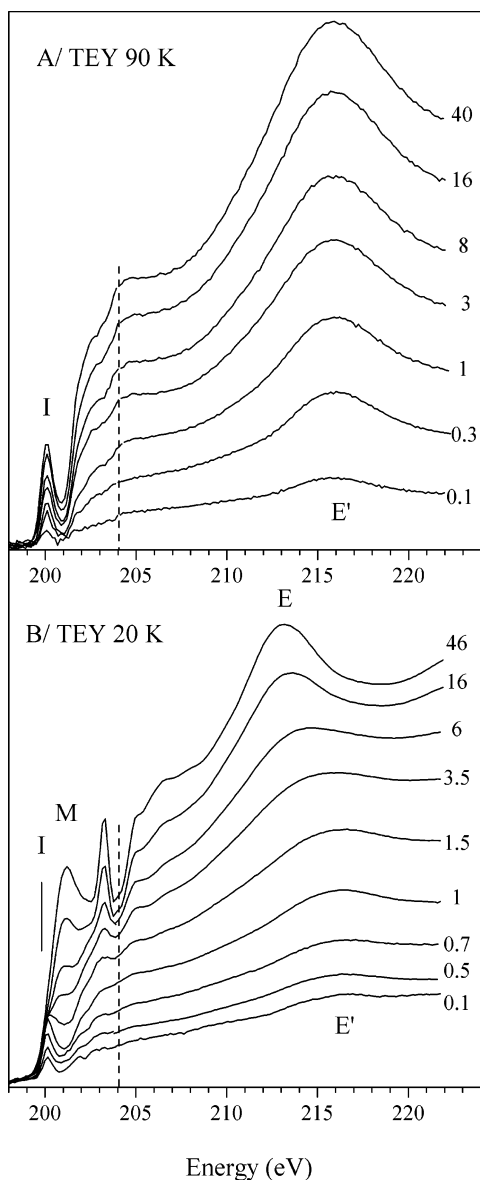


Figure 2. Cl₂p NEXAFS spectra recorded in TEY (bulk signal) at 90 K (panel A) and 20 K (panel B) for increasing HCl exposures on crystalline water ice film (100 langmuir deposited at 150 K). The numbers on the right are the HCl exposures (in langmuir). The spectra are processed for the clarity of the display, with a different scale factor on both sides of the dashed vertical line at 204 eV.

molecules are not concentrated enough to be seen in TEY. Making a linear combination of the Cl⁻ and HCl TEY spectra shown in Figure 1 (curves 1 and 3), we estimate the minimum concentration at which a molecular contribution becomes visible in the Cl⁻ TEY spectrum at about 20%. Since at 20 K and below 1 langmuir no molecular HCl is seen in TEY, we conclude that the concentration of HCl coadsorbed with Cl⁻ does not exceed (and could be well lower than) 20% of the total chlorine uptake.

At 90 K and at any exposure (Figure 3 B), we only observe the chloride anion. No molecular HCl is detected and therefore HCl is fully ionized, as concluded from the TEY results.

(c) The O1s Spectra of Ice. The O1s TEY and PSD spectra of ice are presented in Figure 4. For the TEY data, the shoulder at 535 eV is the 4a₁ orbital.^{40,45} For the PSD signal, this excitation produces an intense peak, shifted to 534.3 eV. This negative shift comes from the decrease of the 4a₁ energy when the number of hydrogen bonds around water is reduced.^{45,46} The 4a₁ energy is then lower in PSD because this method probes

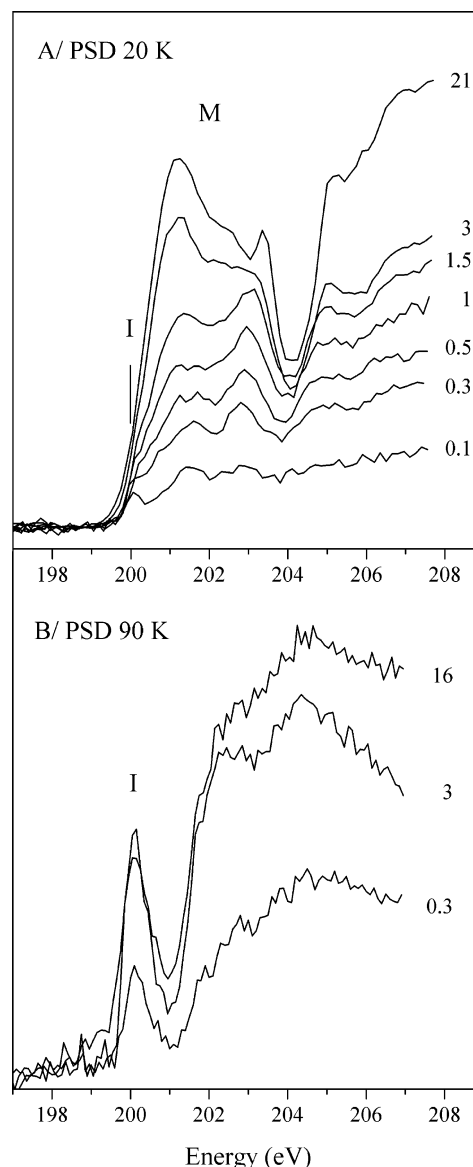


Figure 3. Cl₂p NEXAFS spectra recorded in PSD (surface signal) at 20 K (panel A) and 90 K (panel B) for increasing exposures of HCl on crystalline water ice film (100 langmuir deposited at 150 K). The numbers on the right are the HCl exposures (in langmuir).

the electronic structure of the surface molecules, which naturally possess an incomplete coordination shell. The higher intensity of the 4a₁ in PSD results from the fact that this excitation efficiently breaks the O–H bond, enhancing the ion yield. Last, a key feature of the 4a₁ excitation in the PSD is that the main contributor to its intensity is the ions emitted by the water molecules having one of their two OH bonds directed toward the vacuum, i.e. the molecules having a “dangling” hydrogen atom (the “d-H” groups³⁴).^{40,45,46} The intensity of the 4a₁ resonance in the O1s PSD spectrum is therefore a function of the density of the surface d-H groups.⁴⁵

(d) HCl on Ice at 20 and 90 K: O1s Results. The evolution of the O1s PSD spectra with the HCl exposure is presented in Figure 5. The changes in the 4a₁ intensity are reported in Figure 6. The PSD signal is quickly damped because, when HCl adsorbs on the d-H sites, it obstructs the photodesorption pathways and the ion yield decreases. We see in Figure 6 that the covering of the d-H sites by HCl is faster at 90 K than at 20 K, the ion yield falling to zero for 0.3 langmuir at 90 K and for 1.5 langmuir at 20 K. Last, in a previous study done at 120

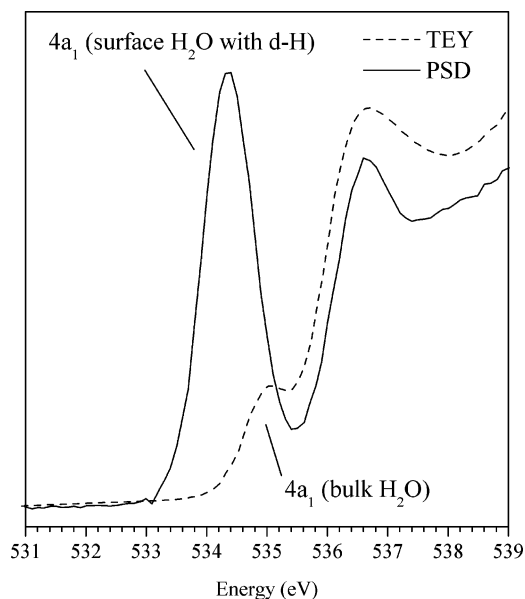


Figure 4. O1s NEXAFS spectra of crystalline ice (100 langmuir deposited at 150 K), recorded in TEY (bulk signal, dashed line) and in PSD (surface signal, full line). The transition to $4a_1$ orbital changes in intensity and energy if the excited water molecule is located in the bulk (TEY) or at the surface (PSD). Only the surface molecules with dangling hydrogen efficiently contribute to the PSD signal, which is therefore proportional to the density of dangling hydrogen bonds (d-H).

K,³⁷ we have observed a partial reconstruction of the PSD signal with time, due to the diffusion of Cl^- into ice. This was not seen here, and we conclude that Cl^- does not incorporate into ice at those temperatures.

(e) HCl on Ice at 20 and 90 K: Evolution of the Chlorine Uptake with the Exposure. The intensity of the $\text{Cl}2p$ TEY spectrum reveals the chlorine uptake. It has been measured at 207 eV (on the raw data) for each exposure and plotted in Figure 7. The 0–1 langmuir exposure range is also detailed in the inset. These results show that the uptake increases with the exposure and saturates. They also show that the uptake at saturation is lower at 90 K than at 20 K.

At 20 K, the molecular multilayer grows as HCl is supplied. At this temperature, the TEY signal saturates when the layer thickness is on the order of the electron mean free path (~ 50 Å). This is not the cause of the saturation at 90 K; otherwise, the maximum value would be the same at the two temperatures. Saturation at 90 K therefore originates from the end of the adsorption process at a certain coverage, θ_{sat} . The ratio of the TEY intensity at each exposure with that measured at θ_{sat} gives the fraction of covered surface with respect to the saturation. This fraction is $0.1\theta_{\text{sat}}$ at 0.1 langmuir, $0.15\theta_{\text{sat}}$ at 0.2 langmuir, $0.2\theta_{\text{sat}}$ at 0.3 langmuir, $0.36\theta_{\text{sat}}$ at 1 langmuir, and $0.65\theta_{\text{sat}}$ at 3 langmuir.

4. Discussion

The $\text{Ih}[0001]$ surface of ice is made of water hexagons forming a bilayer. Those hexagons are made of water molecules with dangling hydrogen (the d-H molecules) or dangling oxygen (the “d-O” molecules) and of water molecules fully coordinated (the “s-4” molecules).³⁴ In a recent model proposed by Bolton et al.,^{9–11} ionization of HCl occurs on ice Ih at the center of relaxed water hexagons in a configuration where the chloride ion has three hydrogen-bonds (“H-bonds”) with two d-H and one d-O water molecules. Ab initio calculations on water clusters led also to the conclusion that three H-bonds are required for

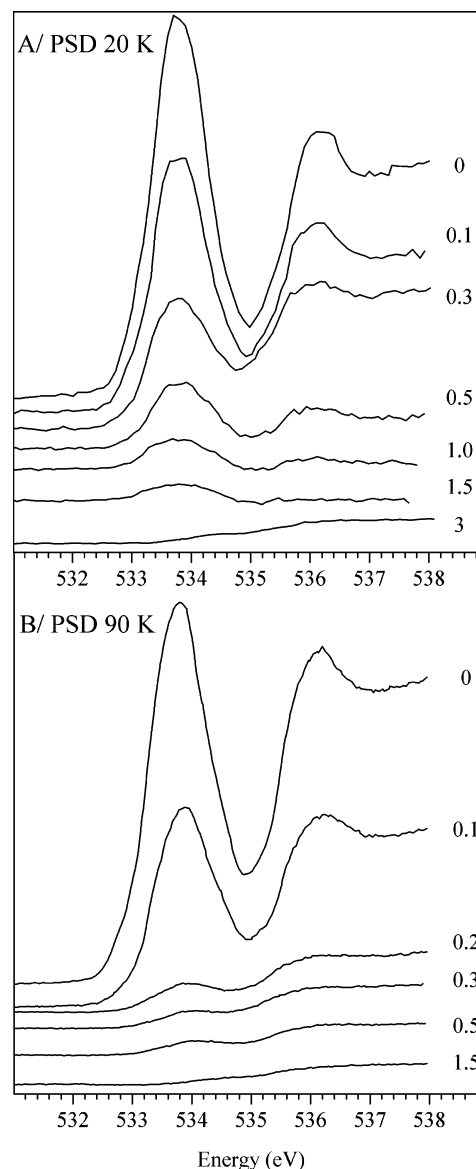


Figure 5. O1s NEXAFS spectra of crystalline water ice (100 langmuir deposited at 150 K) recorded in PSD (surface signal) at 20 K (panel A) and 90 K (panel B), for increasing exposures of HCl. The numbers on the right are the HCl exposures (in langmuir).

the HCl dissociation/solvation.^{12,13,18,19} Once these dangling groups are bound to the chloride ion, none of the six neighboring hexagons have the two free d-H sites required for further HCl ionizations, limiting the composition of the surface hydrate to the hexahydrate $\text{HCl} \cdot (\text{H}_2\text{O})_6$. This composition corresponds to a concentration of chloride anions of $0.18 \times 10^{15} \text{ Cl}^- \text{ cm}^{-2}$.

(a) Results at 90 K. The O1s PSD data (Figure 5 A) indicate that the d-H groups available on the bare surface are all bound to Cl^- at 0.3 langmuir of exposure. If hydrogen bonding with the surface dangling groups is required for ionization and solvation of HCl, this process will then stop at 0.3 langmuir. This is not the case here, since at 0.3 langmuir the amount of chloride anion corresponds only to $0.2\theta_{\text{sat}}$, i.e., 20% of the Cl^- uptake capacity of the ice surface. *This indicates that ionization continues although all the native d-H sites have been used.*

Haq et al.²⁰ have shown that the sticking probability S of HCl on ice at 90 K is 0.97(2) below 0.5 langmuir and then drops to zero as the surface saturates. A sticking probability of 0.91(6) in the 100–125 K range has also been reported.²⁸ Taking $S = 0.97$, we calculate the number of adsorbed chlorine (sticking

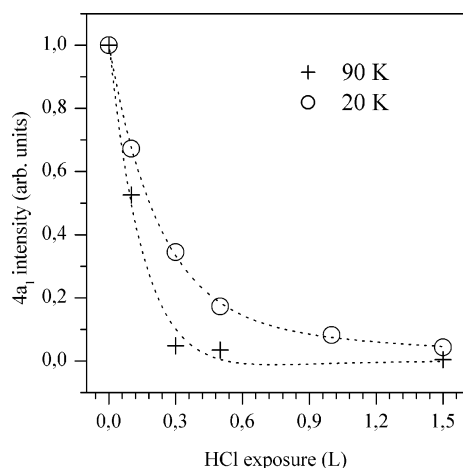


Figure 6. Evolution of the intensity of the $4a_1$ resonance in the O1s PSD spectra (presented Figure 5) with the HCl exposure (in langmuir), at 90 K (+) and 20 K (O). The intensity is measured at the maximum of the $4a_1$ transition and divided by the intensity measured on the uncovered surface. The dashed lines are the polynomial fits of the experimental data to serve as a guide.

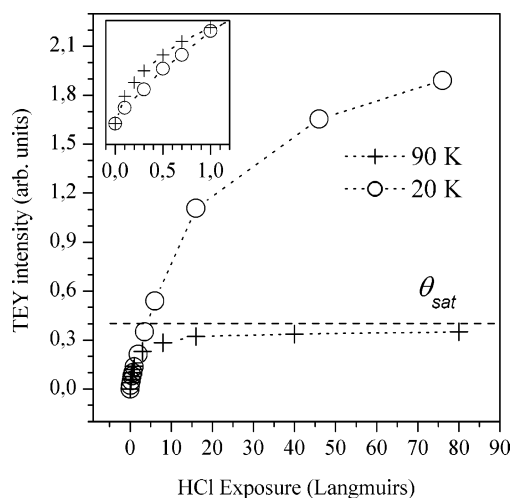


Figure 7. Evolution of the intensity of the unprocessed Cl_{2p} TEY spectra with the HCl exposure (in langmuir), at 90 K (+) and 20 K (O). The intensity is measured at 207 eV. The horizontal dashed line indicates that the HCl coverage at 90 K converges to a saturation value θ_{sat} . The inset details the 0–1 langmuir range.

probability \times exposure time \times HCl flux)⁴⁷ to be $0.18 \times 10^{15} \text{ Cl}^- \text{ cm}^{-2}$ at 0.3 langmuir of HCl ($0.2\theta_{\text{sat}}$). Since the TEY intensity is directly proportional to the chlorine uptake, we deduce from this value the saturation coverage $\theta_{\text{sat}} = 0.18 \times 10^{15}/0.2 = 0.9 \times 10^{15} \text{ Cl}^- \text{ cm}^{-2}$, in good agreement with the saturation concentration of $1.1 \times 10^{15} \text{ Cl}^- \text{ cm}^{-2}$ reported in ref 20. At saturation, the surface hydrate has therefore the concentration of the monohydrate $\text{HCl} \cdot \text{H}_2\text{O}$, a composition also reported in other studies.^{22,26} The calculated uptake of $0.18 \times 10^{15} \text{ Cl}^- \text{ cm}^{-2}$ at 0.3 langmuir—when all the d-H sites are blocked—also matches exactly the maximum composition of the hexahydrate predicted by Bolton ($0.18 \times 10^{15} \text{ Cl}^- \text{ cm}^{-2}$). Thus, the chlorine concentration deduced either from the rate of absorption or from the coverage at which the d-H bonds disappear corresponds to the formation of a surface hexahydrate $\text{HCl} \cdot (\text{H}_2\text{O})_6$. This is consistent with the predicted mechanism of hydrogen bonding with the native dangling groups; we call this mechanism “mechanism I”. Ionization then proceeds despite the depletion of the d-H groups through a further mechanism—“mechanism II”—up to the formation of a surface monohydrate at saturation.

We have noticed previously that we do not observe any regeneration of the O1s PSD signal with time. This shows that no d-H groups reappear after the HCl adsorption, and so the chloride ions remain at the surface and does not incorporate into the lattice. Mechanism II therefore starts on the surface of the hexahydrate, which at first does not have any dangling bonds. Assuming that hydrogen-bonding of HCl with the water molecules is at the origin of ionization in mechanism II, new dangling d-O and d-H groups must be available once all the native ones have been consumed after mechanism I. Above 120 K, it has been observed that the HCl ionization induces the disruption of the hydrogen bonds between water molecules, causing the incorporation of Cl^- into ice to form various bulk HCl hydrates.^{17,20,22,23,27,31,32} At 90 K, this certainly does not occur to this extent, since no chlorine diffusion into the bulk is observed. However, such perturbations can exist, but they are limited to the very surface around the adsorbed Cl^- . Indeed, an extensive relaxation of the ice lattice upon HCl ionization is predicted, with pronounced contraction of the central hexagon around the chloride anion, distortions which are even necessary for ionization.^{9,11} The hydrogen bonding between the surface water molecules is therefore strongly disturbed during phase I, the chloride anions weakening the H-bonds between the water molecules of their solvation shell and the water molecules beyond. The weakening of the hydrogen-bonding network associated with the solvation of protons and Cl^- has been recently invoked as a cause of change in the electron stimulated desorption yield of cations as H^+ , H_2^+ , and $\text{H}^+(\text{H}_2\text{O})_n$ ($n = 1-8$) from low-temperature water ice surfaces covered with a small amount of HCl.⁴⁸ We suggest that the weakening of the surface H-bond lattice allows the water molecules not bound to the chloride anions to solvate further incoming HCl impinging the neighboring hexagons. A possible scenario for the HCl ionization in phase II is therefore the following: (1) the adsorption of a chloride anion in phase I induces surface perturbations, which create loosely H-bound water molecules in a situation where almost no energy is required for the disruption of one or several of their H-bonds with the neighboring water molecules; (2) upon the HCl uptake, those loosely bound water molecules dynamically flip to a geometry where they provide efficient dissociation/solvation conditions for HCl, and their participation in the solvation shell then stabilizes their internal energy by gaining a H-bond with the chloride anion.

(b) Results at 20 K. Our results have shown that HCl dissociates on ice even at 20 K, in good agreement with the prediction of a barrierless ionization.^{9,10,12,13} At low exposures (0–1 langmuir), some molecular HCl is also adsorbed at the side of Cl^- anions, although numerous ionizing sites with d-H bonds are available in this exposure range (Figure 5 A). We suppose that this is a consequence of a reduced surface mobility of the adsorbate. HCl physisorbs or ionizes, depending on the number of dangling bonds available at the adsorption site where the molecule impinges.

At 20 K and before the multilayer condensation prevails (≤ 1 langmuir), ionization is still a very efficient process. When neglecting the contribution of the molecular adsorption (at most 20%), the concentration of chloride anion at 1 langmuir is about the same than at 90 K at 1 langmuir (Figure 7, inset). It is 1.7 times more concentrated than in the hexahydrate and then overtakes the limit of concentration expected when all the native dangling bonds have been consumed. This indicates that ionization has taken place without the native d-H sites, and thus mechanism II also exists at 20 K. In addition, the fact that the d-H groups are still observed at 1 langmuir shows that process

II takes place even before process I is achieved. Again, this is the consequence of the hindrance of the adsorbate translations, which makes the filling of adsorption sites a random process. When HCl adsorbs on a free water hexagon, ionization occurs via mechanism I. If a further molecule impinges on one of the six surrounding hexagons around this site, it stays there and ionizes through mechanism II.

If the dissociation through mechanism I is likely barrierless, it may be also the case for mechanism II. Since we have measured almost the same chloride ion concentration at 20 K and at 90 K below 1 langmuir (Figure 7, inset), the ionization probability of HCl on ice is similar at 20 and 90 K. Temperature is certainly a key parameter for the hopping of HCl from one site to another, but the influence of temperature on the ionization rate at submonolayer coverage was not detected.

Ionization of HCl at low temperature can also occur through a "self-solvation" state, where HCl solvates an adsorbed chloride anion as efficiently as a water molecule.^{18,19} If the molecular contribution observed at 20 K in PSD below 1 langmuir (Figure 3A) is all coming from the HCl species solvating Cl^- , then they cannot exceed 20% of the total chlorine concentration, as deduced from the fact that no molecular HCl is seen in TEY at those coverages (see 3-b-PSD). Therefore, the self-solvation process cannot be at the origin of more than $0.2/0.8 = 25\%$ of the observed ionization events, taking one HCl solvating one Cl^- .¹⁸ If it exists, the self-solvation process has a limited influence on the ionization rate.

Finally, the role of the surface temperature (below the penetration threshold) is mainly to activate the translational motion of the adsorbate between sites and to prevent (at 90 K) or to allow (at 20 K) stable physisorption (self-solvation) states, but those results show that ionization of HCl on ice is possible even at 20 K.

5. Conclusion

Using PSD-NEXAFS, a technique sensitive to the very surface and to the HCl adsorption state, we conclude unambiguously that HCl ionizes on the water ice surface at temperatures as low as 20 K. It occurs by H-bonding with the surface dangling groups ("mechanism I"), likely spontaneously. Comparison between the rate of saturation of the d-H groups and the chlorine uptake indicates that hydrogen bonding of HCl with the native surface groups only accounts for a small part of the chloride anion uptake. Thus, *most of the HCl ionization is achieved on the ice surface without bonding with the native surface dangling groups*. We suggest that the rest of the ionization events take place through a process ("mechanism II") based on the dynamic flipping of water molecules catalyzed by the weakening of the surface of the ice lattice induced by the early dissociation of HCl. This emphasizes the necessity of taking into account not only a single dissociation event but its catalyzing effect on the subsequent events when modeling the uptake of HCl on ice (and likely for many other H-bonding molecules).

At 20 K (but not at 90 K) some molecular species also exists at the side of the ionized chloride anions, physisorbed and/or possibly acting as solvating species. Below 1 langmuir, the adsorbed HCl layer consists essentially of Cl^- , of some molecular HCl (less than 20%), and of some water sites remaining uncovered. As the exposure increases, a layer of condensed HCl grows over this almost ionic surface layer.

At 90 K, HCl is always ionized. Condensation of molecular species is not possible. Taking a sticking coefficient of $S = 0.97$, the concentration of the chlorine hydrate layer at the end of mechanism I is that of $\text{HCl} \cdot (\text{H}_2\text{O})_6$, in agreement with the

limit of concentration predicted in the model of mechanism I proposed by Bolton et al.^{9,10} Mechanism II is by far dominant, since it is responsible for 80% of the ionization events when the saturation is reached. At this stage, the concentration of the hydrate layer is that of the monohydrate $\text{HCl} \cdot \text{H}_2\text{O}$.

References and Notes

- (1) Farman, J. C.; Gardiner, B. G.; Shanklin, J. D. *Nature* **1985**, *315*, 207.
- (2) Solomon, S.; Garcia, R. R.; Rowland, F. S.; Wuebbles, D. J. *Nature* **1986**, *321*, 755.
- (3) Molina, M. J.; Tso, T. L.; Molina, L. T.; Wang, F. C. *Science* **1987**, *238*, 1253.
- (4) Gertner, B. J.; Hynes, J. T. *Science* **1996**, *271*, 1563.
- (5) Estrin, D. A.; Kohanoff, J.; Laria, D. H.; Weht, R. O. *Chem. Phys. Lett.* **1997**, *280*, 280.
- (6) Re, S.; Osamura, Y.; Suzuki, Y.; Shaefer III, H. F. *J. Chem. Phys.* **1998**, *109*, 973.
- (7) Bussolin, G.; Casassa, S.; Pisani, C.; Ugliengo, U. *J. Chem. Phys.* **1998**, *108*, 9516.
- (8) Wang, L.; Clary, D. C. *J. Chem. Phys.* **1996**, *104*, 5663.
- (9) Svanberg, M.; Petterson, J. B. C.; Bolton, K. *J. Phys. Chem. A* **2000**, *104*, 5787.
- (10) Bolton, K.; Petterson, J. B. C. *J. Am. Chem. Soc.* **2001**, *123*, 7360.
- (11) Bolton, K. *J. Mol. Struct. (THEOCHEM)* **2003**, *632*, 145.
- (12) Mantz, Y. A.; Geiger, F. M.; Molina, L. T.; Molina, M. J.; Trout, B. L. *J. Phys. Chem. A* **2001**, *105*, 7037.
- (13) Mantz, Y. A.; Geiger, F. M.; Molina, L. T.; Molina, M. J.; Trout, B. L. *Chem. Phys. Lett.* **2001**, *348*, 285.
- (14) Delzeit, L.; Rowland, B.; Devlin, J. P. *J. Phys. Chem.* **1993**, *97*, 10312.
- (15) Delzeit, L.; Powell, K.; Uras, N.; Devlin, J. P. *J. Phys. Chem. B* **1997**, *101*, 2327.
- (16) Uras, N.; Rahman, M.; Devlin, J. P. *J. Phys. Chem. B* **1998**, *102*, 9375.
- (17) Uras-Aytemiz, N.; Joyce, C.; Devlin, J. P. *J. Phys. Chem. A* **2001**, *105*, 10497.
- (18) Buch, V.; Sadlej, J.; Uras-Aytemiz, N.; Devlin, J. P. *J. Phys. Chem. A* **2002**, *106*, 9374.
- (19) Devlin, J. P.; Uras, N.; Sadlej, J.; Buch, V. *Nature* **2002**, *414*, 269.
- (20) Haq, S.; Harnett, J.; Hodgson, A. *J. Phys. Chem. B* **2002**, *106*, 3950.
- (21) Horn, A. B.; Chester, M. A.; McCoustra, M. R. S.; Sodeau, J. R. *J. Chem. Soc., Faraday Trans.* **1992**, *88*, 1077.
- (22) Bahnam, S. F.; Sodeau, J. R.; Horn, A. B.; McCoustra, M. R. S.; Chester, M. A. *J. Vac. Sci. Technol. A* **1996**, *14*, 1620.
- (23) Graham, J. D.; Roberts, J. T. *Chemometr. Intell. Lab. Syst.* **1997**, *37*, 139.
- (24) Kang, H.; Shin, T. H.; Park, S. P.; Kim, I. K.; Han, S. J. *J. Am. Chem. Soc.* **2000**, *122*, 9842.
- (25) Graham, J. D.; Roberts, J. T. *J. Phys. Chem.* **1994**, *98*, 5974.
- (26) Sadtchenko, V.; Giese, C. F.; Gentry, W. R.; *J. Phys. Chem. B* **2000**, *104*, 9421.
- (27) Harnett, J.; Haq, S.; Hodgson, A. *Surf. Sci.* **2003**, *532–535*, 478.
- (28) Isakson, M. J.; Sitz, G. O. *J. Phys. Chem. A* **1999**, *103*, 2044.
- (29) Andersson, P. N.; Nagard, M. B.; Petterson, J. B. C. *J. Phys. Chem. B* **2000**, *104*, 1596.
- (30) Flückiger, B.; Chaix, L.; Rossi, M. J. *J. Phys. Chem. A* **2000**, *104*, 11739.
- (31) Livingston, F. E.; George, S. M. *J. Phys. Chem. A* **2001**, *105*, 5155.
- (32) Foster, K. L.; Tolbert, M. A.; George, S. M. *J. Phys. Chem. A* **1997**, *101*, 4979.
- (33) Lu, Q. B.; Sanche, L. *J. Chem. Phys.* **2001**, *115*, 5711.
- (34) Devlin, J. P.; Buch, V. *J. Phys. Chem.* **1995**, *99*, 16534.
- (35) Casassa, S. *Chem. Phys. Lett.* **1999**, *321*, 1.
- (36) Clary, D. C.; Wang, L. *J. Chem. Soc., Faraday Trans.* **1997**, *93*, 2763.
- (37) Bournel, F.; Mangeney, C.; Tronc, M.; Laffon, C.; Parent, P. *Phys. Rev. B* **2002**, *65*, 201404.
- (38) Brown, D. E.; George, S. M.; Huang, C.; Wong, E. K. L.; Rider, K. B.; Scott Smith, R.; Kay, B. D. *J. Chem. Phys.* **1996**, *100*, 4988.
- (39) Nakao, F. *Vacuum* **1975**, *25*, 431.
- (40) Coulman, D.; Puschmann, A.; Höfer, U.; Steinrück, H.-P.; Wurth, W.; Feulner, P.; Menzel, D. *J. Chem. Phys.* **1990**, *93*, 58.
- (41) Feulner, P.; Menzel, D. *Laser Spectroscopy and Photochemistry on Metal Surfaces*; Dai, H.-L., Ho, W., Eds.; Advanced Series in Physical Chemistry; World Scientific Publishing: Singapore, 1995; Part II, Vol. 5, p 627.
- (42) Bournel, F.; Mangeney, C.; Tronc, M.; Laffon, C.; Parent, Ph. *Surf. Sci.* **2003**, *528*, 224.

- (43) Stöhr, J. *NEXAFS Spectroscopy*; Gomer, R., Ed.; Springer Series in Surface Sciences; Springer-Verlag: Berlin; Vol. 25, p 239.
- (44) Björneholm, O.; Sundin, S.; Svensson, S.; Marinho, R. R. T.; Naves de Brito, A.; Gel'mukhanov, F.; Ågren, H. *Phys. Rev. Lett.* **1997**, 79, 3150.
- (45) Parent, Ph.; Laffon, C.; Mangeney, C.; Bournel, F.; Tronc, M. *J. Chem. Phys.* **2002**, 117, 10842.

- (46) Cavalleri, M.; Ogasawara, H.; Pettersson, L. G. M.; Nilsson, A. *Chem. Phys. Lett.* **2002**, 364, 363.
- (47) Atkins, P. W. *Physical Chemistry*, 5th ed.; Oxford University Press: Oxford; p 993.
- (48) Herring, J.; Aleksandrov, A.; Orlando, T. M. *Phys. Rev. Lett.* **2004**, 92, 187602–1.